Personalisation of Action Potentials Based on Activation Recovery Intervals in Post Infarcted Pigs: A Simulation Study

Jairo Rodríguez-Padilla[1,2], Rafael Silva[1], Buntheng Ly[2], Mihaela Pop[3], Maxime Sermesant[1,2]

[1]Centre Inria d'Université Côte d'Azur, Sophia Antipolis, France,
[2]IHU-Liryc Université de Bordeaux, Bordeaux, France
[3]Sunnybrook Research Institute, Toronto, Canada

Abstract

Cardiac modeling is a powerful and robust tool in electrophysiology (EP), supporting non-invasive arrhythmia diagnosis and therapy planning. Some studies showed that in silico modeling can be used to predict scar-related arrhythmia risk and ablation targets. However, model personalisation still relies on "average" EP parameters derived from literature, largely due to a paucity of their identification from EP data. We posit that activation-recovery interval (ARI), a surrogate for action potential duration (APD), can be extracted from intracardiac electrograms (iEGMs) and used to parameterize models for more accurate AP wave simulations per individual case. In this work we personalised APDs using ARI values extracted from endocardial electro-anatomical maps recorded in sinus rhythm in post-infarcted swine (n=8). We sought to investigate the differences in model parameters needed to calibrate simulated APDs in healthy tissue and border zone, BZ (i.e., arrhythmia substrate) when using an "average" ARI computed from all cases versus those calibrated from ARIs extracted per case. Results showed that average ARIs in healthy tissue and BZ for all cases were 206.12 $\pm$ 50.18 ms and 213.21 $\pm$ 52.1 ms, respectively. This work underlines the importance of model personalisation by case, suggesting that is fundamentally needed to accurately reproduce in silico the experimental observations.

1. Introduction

In the European Union alone, annual incidences of sudden cardiac death (SCD) and out-of-hospital cardiac arrest (OHCA) reach 250,000 and 344,000 cases, respectively [1]. In particular, the risk of SCD following myocardial infarction poses a significantly critical public health problem [2]. In this context, there is a need of developing new effective and non-invasive predictive tools for arrhythmia risk stratification. Thus, a comprehensive understanding of the impact that each arrhythmic substrate component has on the electrophysiological function is necessary for accurate outcome predictions.

Besides the clinical and experimental studies, computer modeling is a powerful, reliable and effective tool that can be used to predict the arrhythmia risk of post-infarction patients as well as the ablation targets, as proposed in recent modelling works [3, 4]. However, model personalization is still relying on "average" EP parameters derived from literature, largely due to a paucity of their identification from EP clinical data. We hypothesize that activation-recovery interval (ARI), a surrogate for action potential duration (APD), can be extracted from intracardiac electrograms (iEGMs) and used to parameterize models for more accurate AP wave simulations per individual case.

In this study we personalised APDs using ARI values extracted from endocardial electro-anatomical maps recorded in sinus rhythm in post-infarcted swine. Specifically, we sought to investigate the differences in model parameters needed to calibrate simulated APDs in healthy tissue and border zone, BZ (i.e., arrhythmia substrate) when using an "average" ARI computed from all cases versus those calibrated from ARIs extracted per each case.

This work presented in this paper underlies the importance of model personalisation by case, suggesting that proper model parameter calibration is fundamentally needed in order to accurately reproduce in silico the experimental observations.

2. Methodology

2.1. Data aquisition and processing

Magnetic resonance (MR) imaging data was obtained from swine (n=8) following 5 weeks of healing after the infarct was created. Cardiac MR images were obtained using a 3D late gadolinium enhanced (LGE) method at 1.4 mm isotropic voxel. The arrhythmic substrate in LGE images was identified as a "border zone", BZ (i.e., having intermediate signal intensity between healthy tissue and

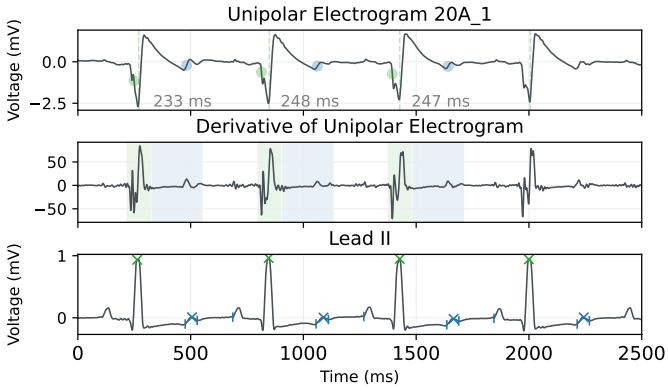

Figure 1. Example of the ARI extraction for a sinus rhythm given iEGM. Top frame: Unipolar signal and the respective activation (green points) and repolarization (blue points) times; Middle frame: derivative of the unipolar shown in the top frame and the shaded area used to look for the activation and repolarization timings; Bottom frame: lead II used for reference and help to define the windows to look for activation and repolarization (crosses).

dense scars). The 3 tissue types (i.e., healthy, BZ, and unexcitable scar) which typically form anatomic reentry circuits, were segmented using a full width at half maximum (FWHM) method as previously described in [5].

The CARTO3 system (J&J, Biosense Webster, USA) was used to perform catheter-based X-ray guided electroanatomical mapping of the LV endocardium for all swine.

ARIs were extracted from the iEGMs using a multilevel discrete wavelet transform (DWT) approach that defines activation and recovery detection windows based on the unipolar signal and surface ECG fiducials. For a more complete description of the extraction algorithm we refer the reader to [6].

Figure 1 shows an example of the ARI extraction for a given unipolar lead.

2.2. Electrophysiological Model

To simulate AP waves, we used a modified version [7] of the Mitchell Schaeffer model [8], whose evolution system is given by the following equations

$$\begin{aligned} \frac{\partial u}{\partial t} &= \nabla \cdot (D\nabla u) + \frac{hu(u-\lambda)(u_{max}-u)}{\tau_{in}} - \frac{u}{\tau_{out}} + J_{stim}(t), \\ \frac{\partial h}{\partial t} &= \epsilon(u,h)\left(h_\infty(u) - h\right), \end{aligned} \tag{1}$$

where

$$\begin{aligned} \epsilon(u,h) &= \frac{1}{\tau_{close}} + \frac{\tau_{close}-\tau_{open}}{\tau_{close}\cdot\tau_{open}} h_\infty(u), \\ h_\infty(u) &= \frac{1}{2}\left(1 - sgn(u - u_{gate})\right). \end{aligned}$$

Variables u and h represent the transmembrane voltage (scaled between 0 and 1) and a gating variable. Parameters τ_{in} and τ_{out} control the strength of the inward (primarily sodium and calcium) and outward (mainly potassium) currents. Parameters τ_{open} and τ_{close} are the time constants with which the gate closes and opens and u_{gate} is the change-over voltage. D is the diffusion coefficient, J_{stim} is the external stimulus, u_{max} controls the maximum voltage that the cell can attain and λ controls the excitability.

Time was discretized with the usual forward Euler scheme, whereas space was discretized by means of a modified Adam-Bashford (diffusion part) and Crank-Nicolson (reaction) scheme, respectively. The implementation was carried out in FEniCSx [9–11]. We simulated a 20×02 mm virtual strand of tissue (600 points and 400 P1 quadrilateral elements with a 100 μm edge length) activated by a stimulus applied 10 times at the most left part of the strand every 800 ms, and then computed an average APD on the the right-most part of the strand from the last beat. Parameters $\tau_{in}, \tau_{out}, \tau_{open}$ and u_{gate} were fixed in all simulations (0.03 ms, 0.6 ms, 120 ms and 0.13, respectively). Furthermore, simulated tissue excitability was reduced in the BZ ($\lambda = 0.2, u_{max} = 0.9$, as in [12]) compared to healthy myocardium ($\lambda = 0.01, u_{max} = 1$). Thus, the personalization of each case was performed by modifying τ_{close}.

Figure 2 shows an example of a simulation in the virtual strand where we initially pace it from the left-most part (Frame (A)). Frames (B) through (E) in Figure 2 show the electrical activity in the strand for different time points after the initial stimulus.

Figure 3 shows exemplary APD recordings on the right-most part of the strand.

3. Results

3.1. APD personalization

Average ARIs (mean ± SD) in healthy tissue and BZ for all cases during sinus rhythm were 206.12 ± 50.18 ms (range [163, 278] ms) and 213.21 ± 52.1 ms (range [170, 262] ms), respectively.

Results on the personalization for the APD in sinus rhythm are shown in Figure 4 on both healthy and BZ. Our results show a monotonic increase on the dependance of the APD on the τ_{close} parameter. This is, the larger the APD in question the higher will be the value of τ_{close}. There is a clear linear correlation between the APD and the value of τ_{close} parameter. Although the behavior is the same for both healthy and BZ cases, we observed that the degree of correlation is larger for the case of the BZ (greater slope in the fit line).

Figure 5 shows some examples of the personalized APDs when using the mean values obtained from averaging the values from all data sets (solid lines) as well as the personalized APDs by case (different dashed lines).

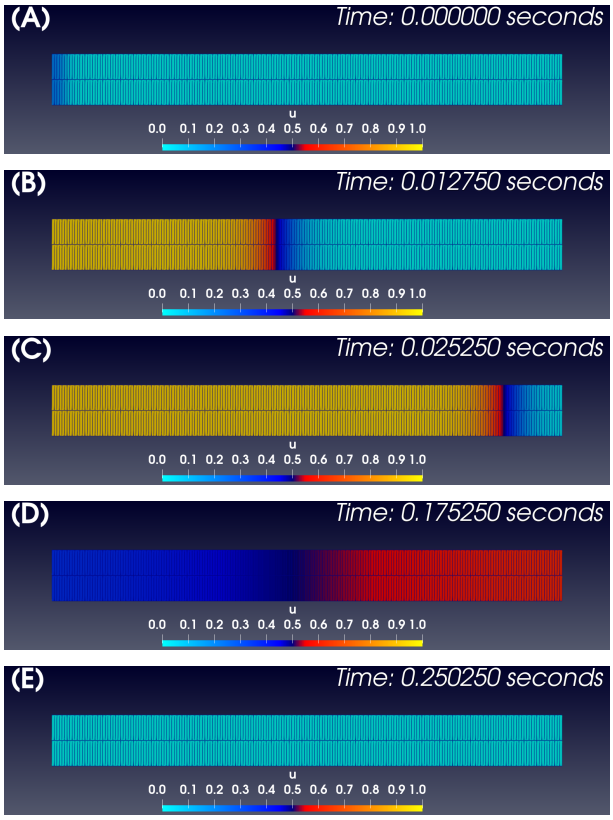

Figure 2. (A): Start of the simulation where we pace the left-most side of the strand and the electrical activity starts to propagate towards the right side. Frames (B)-(D) show the electrical activity on the whole strand at the following time points: $t_1 = 12.75$, $t_2 = 25.25$, $t_3 = 175.25$ and $t_4 = 250.25$ milliseconds after the initial stimulus, respectively.

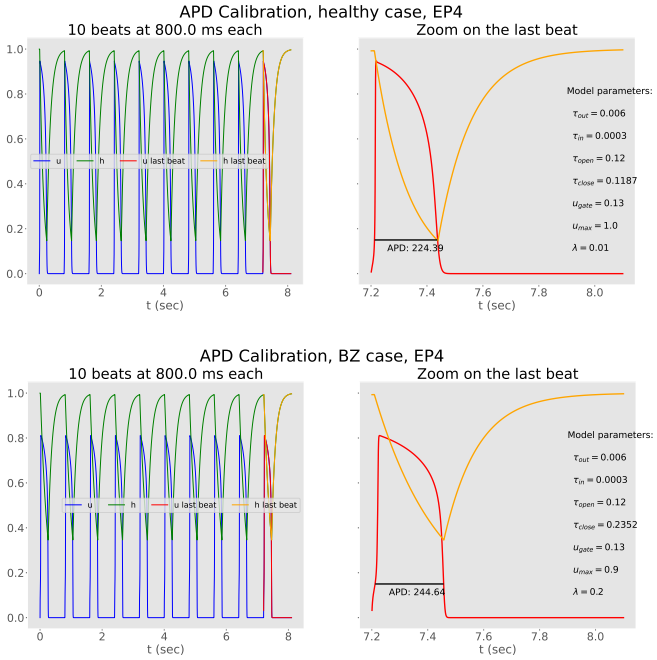

Figure 3. Left frame: APD traces recorded at the right-most part of the strand of tissue simulated; Right frame: Magnified display of the last beat.

3.2. Potential pro-arrhythmic effects

The model personalization of the APD using average values instead of using those calibrated from each individual case, may lead to inaccurate simulation results such as potential false pro-arrhythmic or inhibitory effects. The simulation results showed that the difference in APD values could be up to 65 ms in healthy tissue when the mean value was used for parameter calibration compared to a specific sample in healthy conditions, and up to 49 ms in the BZ. This is a substantial difference which could lead to arrhythmic channels to be exacerbated, specially when performing simulations in tissue.

4. Conclusions

This work underlines and stresses the importance of model personalization by case. Although model personalization done by using average measurements may be valuable for testing different hypotheses, such approach can lead to an inclusion an additional arrhythmic effect that is not necessarily inherent to the data. Thus, we conclude that the personalization by case is fundamentally needed to accurately reproduce in silico the experimental observations.

Current efforts and future developments will be focused on expanding this work to a 3D biventricular heart model and study arrhythmia inducibility via computer simulations.

Acknowledgements

This work was supported by the SimCardioTest project which has received funding from the European Union's Horizon 2020 research and innovation program under grant agreement No. 101016496, by the French government, through the 3IA Côte d'Azur Investments in the Future project managed by the National Research Agency (ANR) with the reference number ANR-19-3IA-0002 and by a Canadian CIHR project grant (PJT) 153212.

References

[1] Empana JP, Lerner I, Valentin E, Folke F, Böttiger B, Gislason G, Jonsson M, Ringh M, Beganton F, Bougouin W, et al. Incidence of sudden cardiac death in the european

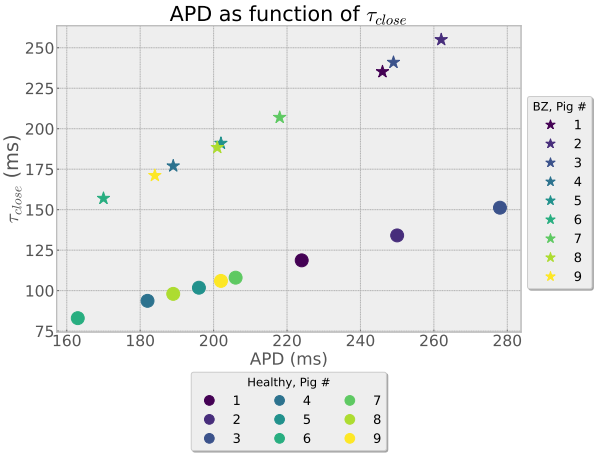

Figure 4. Personalization of APDs varying the τ_{close} parameter for both healthy (circles) and BZ (stars).

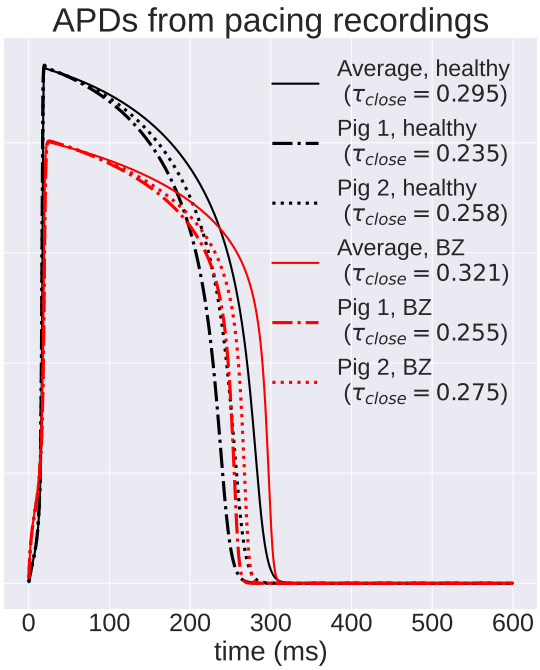

Figure 5. Exemplary cases on the personalization of APDs for both healthy (black) and for the BZ (red).

union. Journal of the American College of Cardiology 2022;79(18):1818–1827.

[2] Fishman GI, Chugh SS, DiMarco JP, Albert CM, Anderson ME, Bonow RO, Buxton AE, Chen PS, Estes M, Jouven X, et al. Sudden cardiac death prediction and prevention: report from a national heart, lung, and blood institute and heart rhythm society workshop. Circulation 2010; 122(22):2335–2348.

[3] Arevalo HJ, Vadakkumpadan F, Guallar E, Jebb A, Malamas P, Wu KC, Trayanova NA. Arrhythmia risk stratification of patients after myocardial infarction using personalized heart models. Nature Communications 2016; 7(1):11437.

[4] Campos FO, Orini M, Arnold R, Whitaker J, O'Neill M, Razavi R, Plank G, Hanson B, Porter B, Rinaldi CA, et al. Assessing the ability of substrate mapping techniques to guide ventricular tachycardia ablation using computational modelling. Computers in Biology and Medicine 2021; 130:104214.

[5] Escartin T, Krahn P, Yu C, Ng M, Barry J, Singh S, Wright G, Pop M. The extent of lge-defined fibrosis predicts ventricular arrhythmia severity: Insights from a preclinical model of chronic infarction. In International Conference on Functional Imaging and Modeling of the Heart. Springer, 2023; 698–707.

[6] Silva R, Rodríguez Padilla J, Pop M, Sermesant M. Automatic analysis of activation recovery interval in heterogeneous fibrotic tissue from chronically infarcted swine. In 2024 Computing in Cardiology Conference (CinC), volume 51. IEEE, 2024; 1–4.

[7] Djabella K, Landau M, Sorine M. A two-variable model of cardiac action potential with controlled pacemaker activity and ionic current interpretation. In 2007 46th IEEE Conference on Decision and Control. IEEE, 2007; 5186–5191.

[8] Mitchell CC, Schaeffer DG. A two-current model for the dynamics of cardiac membrane. Bulletin of Mathematical Biology 2003;65(5):767–793.

[9] Baratta IA, Dean J, Dokken J, Habera M, Hale J, Richardson C, Rognes M, Scroggs M, Sime N, Wells G. Dolfinx: the next generation fenics problem solving environment. preprint, 2023. Accessed February 2024;9.

[10] Scroggs MW, Dokken JS, Richardson CN, Wells GN. Construction of arbitrary order finite element degree-of-freedom maps on polygonal and polyhedral cell meshes. ACM Transactions on Mathematical Software TOMS 2022; 48(2):1–23.

[11] Alnæs MS, Logg A, Ølgaard KB, Rognes ME, Wells GN. Unified form language: A domain-specific language for weak formulations of partial differential equations. ACM Transactions on Mathematical Software TOMS 2014;40(2):1–37.

[12] Cedilnik N, Pop M, Duchateau J, Sacher F, Jaïs P, Cochet H, Sermesant M. Efficient patient-specific simulations of ventricular tachycardia based on computed tomography-defined wall thickness heterogeneity. Clinical Electrophysiology 2023;9(12):2507–2519.

Address for correspondence:

Jesus Jairo Rodríguez Padilla
2004, routes des Lucioles, 06902 Sophia Antipolis Cedex, France.
jesus-jairo.rodriguez-padilla@inria.fr